31st Annual International Conference of the IEEE EMBS
Minneapolis, Minnesota, USA, September 2-6, 2009

Measurements of the Contact Pressure in Human Vocal Folds

Li-Jen Chen and Luc Mongeau

***Abstract*—the contact pressure experienced by human vocal folds during phonation is usually considered as the most likely source of phonotrauma. Direct contact pressure measurements using pressure sensors were attempted, although some interference with vocal folds oscillation was found to occur. A nonintrusive approach for the contact pressure estimation from high speed images was therefore investigated, based on a Hertzian Impact model. A verification study of the accuracy of this method was performed. Results from the nonintrusive approach were compared with results from direct measurements using a physical model of the human vocal folds. The accuracy of the estimated contact pressure from the nonintrusive method was found to be acceptable. Disadvantages and possible sources of error are discussed.**

I. Introduction

VOICE is produced by the flow-induced self-oscillations of the vocal folds. Vocal folds collision during the self-oscillations is commonly observed in clinical studies in the modal register. The contact pressure on the medial surface of the vocal folds during collision is often considered the most likely source of trauma to the vocal fold membrane [1]. The contact pressure and the aerodynamic pressure in the surrounding fluid were measured as a function of prephonatory configurations in one previous study [1]. An excised canine hemilarynx was used since the amplitude and the frequency of vocal fold vibration of a hemilarynx as a function of subglottal pressure were found to be similar to those of a full larynx [2]. The contact pressure on the medial surface was found to vary along the anterior-posterior direction, reaching a peak value on the order of 0.5 ~ 5.0 kPa at the midpoint. A piezoresistive transducer was guided videoendoscopically to measure vocal folds contact pressure in human subjects [3, 4]. The contact pressure amplitude was found to vary between 0.4 to 3.2 kPa. It was noted that accurate direct measurements of the contact pressure in human subjects are hampered by sensor and tether size, sensor sensitivity, and other clinical limitations.

The Digital Image Correlation (DIC) method allows for the measurement of the displacement field on the visible surface of a deformable solid. DIC was found to be an accurate and a promising experimental tool to investigate the deformation of the superior surface of a vocal folds physical model [5]. Displacement and strain fields on the superior surface of a physical model were obtained using DIC [6-8]. Potential application in clinical studies using a high-speed videoendoscopy is presently under investigation. The contact pressure on the medial surface of a physical model was estimated from the displacement and strain data of the superior surface using a Hertzian impact model [8]. This approach is believed to have potential applications in clinical settings. But no verification of this estimation method via direct measurements has been made to date.

The first goal of the present study was to develop a sensor suitable for contact pressure measurements. An exploratory study of the contact pressure in human vocal folds was performed using a probe microphone. The second goal was to investigate the accuracy of the DIC-based approach of contact pressure estimation and the Hertzian impact model. A silicone hemilarynx model was used. To compute contact pressure, superior surface deformation data of the physical model were obtained using DIC. The estimated contact pressure was then compared with that measured using the probe microphone. The nonintrusive approach yielded a satisfactory estimate. Disadvantages and possible sources of error were investigated.

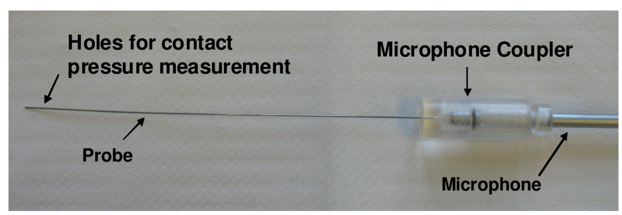

Fig. 1. Schematic of the probe microphone.

II. Methods

A. Design and Verification of the Probe Microphone

The contact pressure sensor was based on a probe microphone. The transducer consisted of a microphone (Brüel & Kjær 4939, 0.635 cm diameter), a 15-cm-long stainless steel capillary probe with an outer diameter of 0.64 mm and an inner diameter of 0.5 mm, and a microphone coupler, as shown in Fig. 1. The microphone had a sensitivity of 4 mV/Pa, with a peak sound pressure of 10 kPa. The size of the probe was selected as a compromise between interference with the vocal fold model oscillations and noise in the recorded data. Smaller probes reduced interference at the expense of a reduced sensitivity because of increased visco-thermal losses, leading to higher noise levels. Several probe diameters were tested, and an optimum value was identified. One end (open

Li-Jen Chen is with the Department of Mechanical Engineering, McGill University, Montreal, QC H2X2P1 Canada (e-mail: li-jen.chen@mail.mcgill.ca).

Luc Mongeau is with Department of Mechanical Engineering, McGill University, Montreal, QC H2X2P1 Canada (corresponding author to provide phone: 514-398-2777; e-mail: luc.mongeau@mcgill.ca).

978-1-4244-3296-7/09/$25.00 ©2009 IEEE

end) of the probe was attached to the microphone coupler, and the other end (closed end) was located subglottally, upstream of the vocal fold model. A hole, located 5 mm away from the close end, was drilled through the probe side-wall. This hole was positioned in the center of the contact region, facing the medial surface of the vocal folds model. The area of the hole was small enough that the vocal fold model fully covered and sealed the hole during collision. It was hypothesized that the air pressure within the contact area was at all time in equilibrium with the local normal surface stress within the vocal fold model solid. The influence of the probe on the contact pressure amplitude was assumed to be negligible.

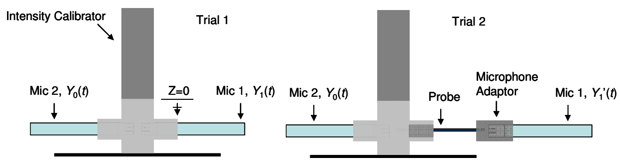

Fig. 2. Schematic of the calibration procedure.

Due to sound wave attenuation and acoustic standing waves in the probe, the pressure data recorded by the microphone was different from the actual pressure at the probe sidewall hole. To compensate for the probe response, the transfer function, $TF(f)$, between the signal from a known linear condenser microphone with uniform response, $Y_1(t)$, and the probe microphone output, $Y_1'(t)$, was determined. Fig. 2 shows a schematic of the transfer function determination. An intensity calibrator (Brüel & Kjær type 3541) was used to generate white noise with a frequency bandwidth of 10k Hz. Microphone 1 was used for the probe microphone, and the Microphone 2 was used as a common reference. The transfer function $TF(f)$ was obtained using

$$TF(f) = \frac{TF_2(f)}{TF_1(f)} = \frac{H_1'(f)/H_0(f)}{H_1(f)/H_0(f)}, \tag{1}$$

where $H_1(f)$, $H_1'(f)$, and $H_0(f)$ are the Fourier Transforms of Microphone 1 signal $Y_1(t)$, probe microphone output $Y_1'(t)$,and Microphone 2 signal $Y_0(t)$, respectively.

Once $TF(f)$ is determined, the corrected pressure data, $\tilde{Y}_1(t)$, was obtained from the measured response, $\tilde{Y}_1'(t)$, by using

$$\tilde{Y}_1(t) = F^{-1}[F[\tilde{Y}_1'(t)]/TF(f)], \tag{2}$$

where $F[\ ]$ and $F^{-1}[\ ]$ are Fourier and Inverse Fourier Transform operator, respectively.

Experiments were performed to establish the accuracy of the probe microphone, as shown in Fig. 3. In the first trial, Microphone 1 and Microphone 2 were mounted 2 cm and 8 cm away from a constant sound pressure generator, respectively. In the second trial, Microphone 1 was replaced by the probe microphone. Using Microphone 2 data in both trials as a common reference, the corrected response of the pressure data obtained using the probe micorphone, $\tilde{Y}_1(t)$, was compared with pressure data obtained using Microphone 1, $Y_1(t)$. Satisfactory agreement was found in both phase and amplitude. All pressure data from the probe microphone were thus treated with a post-processing correction.

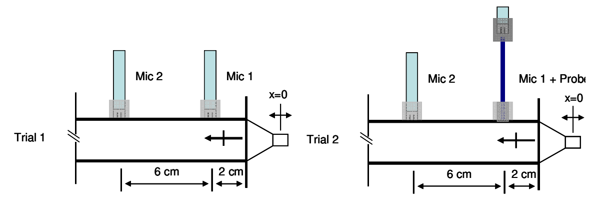

Fig. 3. Schematic of the verification test

B. Non-intrusive contact pressure estimation based on a Hertzian impact model

From a Hertzian impact model [5], the total penetration depth through the contact plane, δ_p, when two deformable bodies contact is

$$\delta_p = \pi a P_c / 2E^*, \tag{3}$$

where a is the equivalent radius of a circular contact region, P_c is the contact pressure, and E^* is the effective modulus. The effective modulus, E^*, is defined as

$$E^* = \frac{1}{\frac{1-\nu_1^2}{E_1} + \frac{1-\nu_2^2}{E_2}}, \tag{4}$$

where E_1 and E_2 are the Young's modulus of the two deformable bodies, and ν_1 and ν_2 are Poisson ratios of the physical model and the acrylic contact wall, respectively. Incompressibility ($\nu_1 = 0.5$) was assumed for the rubber material. Therefore,

$$E_1 = 2G_1(1+\nu_1) = 3G_1, \tag{5}$$

where G_1 is the shear modulus of the silicone rubber. Since the Young's modulus of acrylic is much larger than that of silicone rubbers ($E_2 > 10^6 E_1$), the second term in the denominator of (4) was ignored. Therefore,

$$E^* = 4E_1/3 = 4G_1, \tag{6}$$

and

$$\frac{P_c}{G_1} = \frac{8\delta_p}{\pi a}. \tag{7}$$

The contact area, A, was determined independently. Since the contact area had mild ellipticity, the errors introduced by the use of a circular contact model with an equivalent radius were deemed insignificant [9]. Hence, the equivalent radius of a circular contact region was obtained through

$$a = \sqrt{A/\pi}. \tag{8}$$

The total penetration depth was obtained through extrapolation of the initial strain, assuming that the medial-lateral strain can develop freely without the presence of the side wall [5]. Thus, the penetration depth was obtained using

$$\delta_p = (\tilde{\varepsilon}_{xx} - \varepsilon_{xx})d \,, \tag{9}$$

where d is the depth of the vocal fold model influenced by the contact, $\tilde{\varepsilon}_{xx}$ is the extrapolated medial-lateral strain, and ε_{xx} is the measured medial-lateral strain. Thus, the contact pressure in terms of material properties, extrapolated and measured strains, and contact characteristics is

$$\frac{P_c}{G_1} = \frac{8(\tilde{\varepsilon}_{xx} - \varepsilon_{xx})d}{\pi a} \,. \tag{10}$$

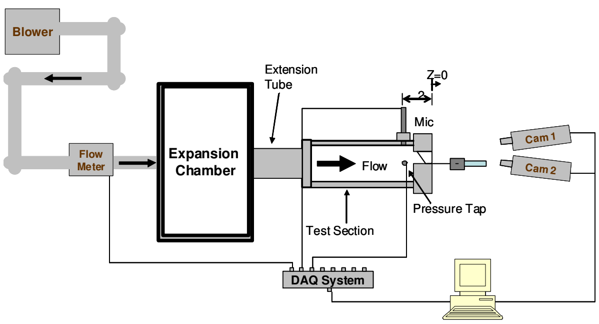

Fig. 4. Experimental apparatus.

C. Experimental Setup and Procedures

A hemilaryx model of human vocal folds was fabricated using silicone rubber. A canonical geometry of the vocal fold, or M5 profile, was used [10]. The fabricated model was mounted on an acrylic clamp with fixed boundary conditions on the anterior, posterior, and lateral surfaces. The physical model was found to have characteristics comparable with human vocal folds from previous studies. Fig. 4 shows a schematic of the test section. More details of the experimental setup can be found in [12].

Model deformation in one oscillation cycle was obtained using two cameras with a constant frame rate of 12 frames/second. Since the oscillation was purely periodic after reaching a steady state, one complete oscillation cycle was constructed by recording images with a fixed phase lag offset from several consecutive cycles.

Air flow was supplied from compressed shop air with adjustable flow rate. The flow rate, Q, was increased gradually. Flow rate values were recorded after the reading stabilized (around 10 seconds in the current study). The contact pressure was recorded at Q = 43.3 and Q = 45.2 L/Min, and RMS acoustic pressure of 0.50 and 0.54 kPa, respectively. A commercially available package (Correlated Solutions Inc.) was used to perform the 3D-DIC analysis.

III. Results

A. Contact pressure estimation using DIC

To estimate the contact pressure using deformation data, a medial strain – flow rate relation, when no vocal folds contact was involved, was required for extrapolation of the feely-developed medial strain at higher subglottal pressures. Unlike full-larynx vocal folds models [5], only two data points prior to vocal folds contact were available for the current model. Fig. 5 shows medial-lateral displacement and stress contour plot at Q = 45.2 L/Min. Using (12), the estimated contact pressures based on superior surface deformation data was 0.63 and 0.74 kPa at Q = 43.3 and Q = 45.2 L/Min, respectively.

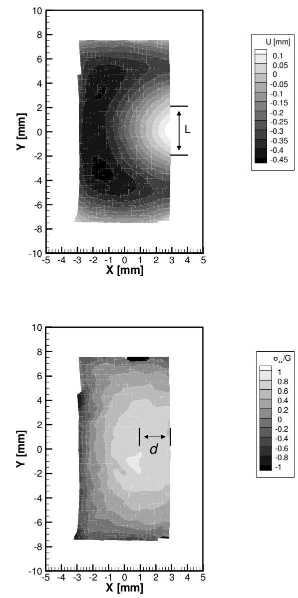

Fig. 5. Contour plots of medial-lateral displacement (left) and stress

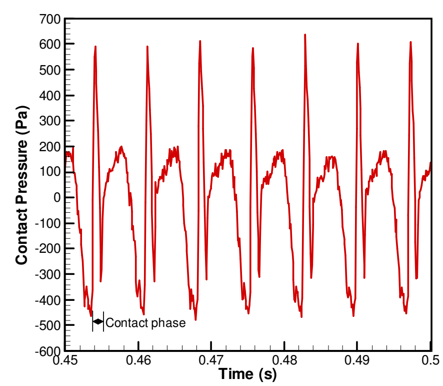

Fig. 6. Time history of the measured contact pressure of the physical model (Q = 45.2 L/Min).

B. Contact pressure measurement using a probe microphone

Fig. 6 shows the time history of the measured contact pressure. The pressure amplitude reached a minimum value immediately prior to contact. The negative pressure might be caused by a negative pressure wave in the flow. Immediately after the contact, the pressure amplitude reached a maximum, followed by rapid oscillations. Note the pressure recorded outside the contact phase was the aerodynamic pressure in the glottis since the hole on the probe was fully exposed to the flow. The peak contact pressure values were $P_{pk} = 0.59$ and $P_{pk} = 0.63$ kPa at $Q = 43.3$ and $Q = 45.2$ L/Min, respectively.

C. Exploratory measurements with human subjects

Exploratory contact pressure measurements using the probe microphone were performed based on subjects. Guided videoendoscopically, the pressure sensor was placed between vocal folds through a channel within a flexible laryngoscope. Since this was an exploratory test, only two tokens were taken, and only one out of two yielded satisfactory results. The time history for the contact pressure is shown in Fig. 7. The peak contact pressure was found to be around 1kPa, which is consistent with previous measurement data [3, 4]. The contact phase was identified with the aid of an electroglottograph signal collected synchronously with the contact pressure. The applicability of the probe microphone concept for in-vivo measurements was deemed satisfactory usage in clinical studies.

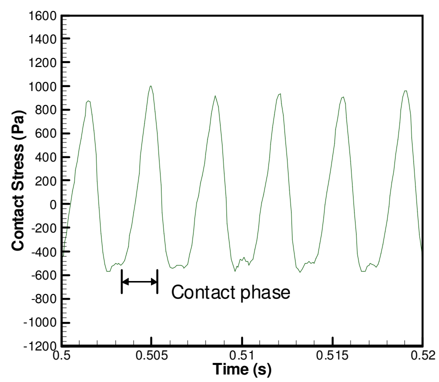

Fig. 7. Time history of the measured contact pressure

IV. Discussion and Conclusion

The results show that the estimated peak contact pressure based on superior surface deformation data obtained using DIC may be slightly overestimated. The error of the estimation reached 6.6% and 17.5 % at $Q = 43.3$ and $Q = 45.2$ L/Min, respectively. The penetration depth, affected by the extrapolation of maximum freely-developing medial strains, was a key parameter to estimate the contact pressure using the Hertzian model. The medial strains extrapolated based on limited data prior to the onset of the contact might be a source of error. Besides, the insufficient temporal resolution of the cameras might also contribute to the error, although hundreds of pictures were taken for a single data point to compensate camera deficiency. Nevertheless, the estimated values of contact pressures were a good first cut estimate.

The estimation of the contact pressure based on superior surface deformation data has great clinical advantages over intrusive measurements. Interferences on vocal folds oscillations due to the presence of measurement devices, such as reduction of orifice area and blockage of vocal folds movements, are irrelevant. More representative and accurate vocal folds oscillation data are available. However, an appropriate dye to apply a speckle pattern for clinical usage is still unavailable. From clinical observations, the glare on the superior surface of vocal folds due to the high intensity light source may largely reduce the area allowable for performing DIC. A high intensity omni-directional light may be needed.

Exploratory contact pressure measurements using a probe microphone were made. Preliminary results support its application in future studies. More studies are underway.

Acknowledgment

This work was supported by the research grants No. R01 DC005788 and R01 DC008290 from the National Institute for Deafness and other Communication Disorders (NIH-NIDCD).

References

[1] J. J. Jiang and I. R. Titze, "Measurement of vocal fold intraglottal pressure and impact stress," *Journal of Voice,* vol. 8, pp. 132-144, 06 1994.

[2] J. J. Jiang and I. R. Titze, "A Methodological Study of Hemilaryngeal Phonation," *Laryngoscope,* vol. 103, pp. 872-882, 1993.

[3] M. M. Hess, K. Verdolini, W. Bierhals, U. Mansmann, and M. Gross, "Endolaryngeal contact pressures," *Journal of voice : official journal of the Voice Foundation,* vol. 12, pp. 50-67, 01/01 1998.

[4] K. Verdolini, M. M. Hess, I. R. Titze, W. Bierhals, and M. Gross, "Investigation of vocal fold impact stress in human subjects," *Journal of voice : official journal of the Voice Foundation,* vol. 13, pp. 184-202, 06/01 1999.

[5] M. Spencer, T. Siegmund, and L. Mongeau, "Determination of superior surface strains and stresses, and vocal fold contact pressure in a synthetic larynx model using digital image correlation," *The Journal of the Acoustical Society of America,* vol. 123, pp. 1089-1103, 2008.

[6] S. Mantha, L. Mongeau, and T. Siegmund, "Dynamic image correlation of a dynamic physical model of the vocal folds," *Adv. Bioeng,* vol. 57, pp. 77-78, 2005.

[7] S. Mantha, T. Siegmund, and L. Mongeau, "Estimation of strain fields in self oscillating physical glottis models using 3D digital image correlation," in *Proceedings of the Fourth International Workshop on Models and Analysis of Vocal Emissions for Biomedical Applications*, Florence, Italy, 2005.

[8] M. Spencer, "Indirect determination of the strain and stress in physical models of the vocal folds using digital image correlation," in *The School of Mechanical Engineering*. vol. MS West Lafayette, IN: Purdue University, 2007.

[9] J. A. Greenwood, "A simplified elliptic model of rough surface contact," *Wear,* vol. 261, pp. 191-200, 2006.

[10] R. C. Scherer, D. Shinwari, K. J. D. Witt, C. Zhang, B. R. Kucinschi, and A. A. Afjeh, "Intraglottal pressure profiles for a symmetric and oblique glottis with a divergence angle of 10 degrees," *The Journal of the Acoustical Society of America,* vol. 109, pp. 1616-1630, 2001.

[11] S. L. Thomson, L. Mongeau, and S. H. Frankel, "Aerodynamic transfer of energy to the vocal folds," *The Journal of the Acoustical Society of America,* vol. 118, pp. 1689-1700, 2005.

[12] L.-J. Chen and L. Mongeau, "Determination of vocal folds deformation fields from flow and superior surface data using finite element analysis," *The Journal of the Acoustical Society of America,* in submission.